Effects of Dynamic Time Slot Scheduling Schemes and Soft Handoff on the Performance of TDD DS CDMA Systems with 2D Rake Receivers over a Nakagami-m Frequency Selective Fading Channel

Roger Pierre Fabris Hoefel and Celso de Almeida
DECOM- FEEC – State University of Campinas
C.P. 6.101 - Campinas - 13.081-970 - Brazil
rogerhoefel@uol.com.br, celso@decom.fee.unicamp.br

Abstract – In this paper[1], we derived analytical expressions to assess the performance of Time Division Duplexing (TDD) Direct Sequence Code Division Multiple Access (DS-CDMA) systems with coherent bi-dimensional (*2D) Rake receivers. These results are used in the performance comparison between coherent and optimum 2D Rake receivers It is also shown that soft handoff allows gains of 2 dB in the Signal-to-Interference-plus-Noise-Ratio (SINR) at the 2D Rake receiver output. Finally, we also show that dynamic time slot allocation schemes allow considerable performance gains of users' (SINR) and network operators' (throughput multiplication) point of view.*

I – Introduction

Considering a multitude of parameters, we have concluded that the time variant and irregular spatial-temporal channel characteristics have a strong influence on the performance of TDD DS-CDMA systems with 2D RAKE receivers [1-2]. In this paper, besides to developed analytical expressions to evaluate the performance of coherent 2D Rake receivers over Nakagami-m frequency selective fading channels, we will also show that dynamic time slot allocation algorithms can improved substantially the uplink performance of TDD DS-CDMA systems with wavefield transceivers.

This paper has been organized as follows. A description of the 2D Rake receiver is presented in Section II. Analytical expressions to estimate the performance of the coherent 2D Rake receiver are developed in Section III. A brief description of a network simulator is done in Section IV. A comparison between analytical and simulation results is carried out in Section IV. The effects of soft handoff and dynamic time slot scheduling on the system performance are investigated in Section VI and VII, respectively. Finally, the conclusions are done in Section VIII.

II - 2D Rake Receiver

The 2D Rake receiver, constituted of an array of M antennas and P taps per antenna, reduces interference by means of spatial and temporal processing in order to produce an improved decision variable to the detection circuit. A description of 2D Rake receiver can be found in [3, pp. 81]. At this section, we are going to present the steps to estimate numerically the SINR at the 2D Rake receiver output.

Assuming a chip and phase synchronous system, the SINR for the *k-th* user in a interference limited coherent binary phase shift keying (BPSK) DS-CDMA system can be estimated by [4, pp. 40]:

$$\mathrm{SINR}_k = \frac{G_p \mathbf{W}_k^H \mathbf{R}_{s,k} \mathbf{W}_k}{\mathbf{W}_k^H \mathbf{R}_{u,k} \mathbf{W}_k}, \quad (1)$$

where G_p is the processing gain; $\mathbf{W}_k$ is a column vector that contains the MP coefficients of the 2D Rake receiver for the *k-th* target user; $\mathbf{R_{s,k}}$ is the desired signal covariance matrix, $\mathbf{R_{u,k}}$ is the multiple access interference (MAI) plus noise covariance matrix observed by the *k-th* user; and $(.)^H$ represents the Hermitian operation.

Assuming a frequency selective fading channel with inbound diversity L and negligible intersymbolic interference ($L<<G_p$), then the *k-th* user´s M by L channel matrix can be stated as:

$$\mathbf{H}_k = [\mathbf{h}_{k,0}\ \mathbf{h}_{k,1} \cdots \mathbf{h}_{k,L-1}], \quad (2)$$

where $\mathbf{h}_{k,l}$ is the M column vector that models the arrival at the antenna array of *l-th* multipath of the *k-th* user.

For a linear equally spaced (LES) array with M correlated antennas (i.e. the number of spatial diversity branches M_D is equal to 1) separated by half-wavelength of frequency carrier, the steering vector is given by:

$$\mathbf{h}_{k,l} = \sqrt{P_{k,l}}\alpha_{k,l}[1\ e^{j\pi\sin\theta_{k,l}} \cdots e^{j(M-1)\pi\sin\theta_{k,l}}]^T, \quad (3)$$

where $\alpha_{k,l}$ is a complex random variable (RV) that models the channel gain for the *l–th path* of *k-th* user, and $\theta_{k,l}$ is the Direction-of-Arrival (DOA) for the *l–th* path of the *k-th user*.

If the multipath fading is uncorrelated in all antenna elements (i.e. M_D=M), then the spatial temporal signature can be rewritten as:

$$\mathbf{h}_{k,l} = \sqrt{P_{k,l}}[\alpha_{k,l,0} \cdots \alpha_{k,l,M-1}]^T, \quad (4)$$

where $\alpha_{k,l,m}$ is a complex RV that models the channel gain for k-th user at the *l–th* path at the *m-th* antenna element.

The second moment of channel gain per antenna is normalised, i.e.

$$\sum_{l=0}^{L-1} E\left[\left|\alpha_{k,l,m}\right|^2\right] = 1 \ \text{ for } m = 0, \cdots, M-1. \quad (5)$$

Therefore, $P_{k,l}$ models the average power per antenna received by the *k-th* user at *l-th* path. Take into consideration the following reasoning: *(i)* the slow power control loop (PCL) compensates perfectly the attenuation due to the assumed log-linear long-term propagation model with path loss exponent, Γ, and log-normal shadowing with standard deviation σ_{dB}; *(ii)* the mobile stations (MSs) select the BS which requires the minimum average transmission power. Hence, the average receive power per antenna given by

[1] This work was subsidized by *Ericsson Telecommunications S.A* under Ericsson/UNICAMP contract no. 17/00. R.P.F. Hoefel is not employed by UNICAMP or Ericsson

$$P_k = \sum_{l=0}^{L-1} P_{k,l}\,, \qquad (6)$$

is equal to one when the MS is controlled by the target BS, and P_k is a function, among other parameters, of user spatial location, path loss and log-normal shadowing when this MS contributes with external MAI to the target cell [5]. It was also assumed that the same average power is received in all antennas of each sector.

Noticing that the solution that minimizes the mean square error (MSE) of chip sequence also minimizes the MSE of symbol sequence estimatation [3, pp. 89], then the spatial covariance matrix (dimension MP by MP) of interference-plus-noise can be stated as:

$$\mathbf{R} = \sum_{j=1}^{KN_{BS}} H_j H_j^H + \sigma_n^2 \mathbf{I}_{MP}\,, \qquad (7)$$

where K is the number of MSs physically located in each of one of N_{BS} hexagonal BSs, and the AWGN power in a bandwidth W is $2\sigma_n^2 W$, where $N_o=2\sigma_n^2$ is the noise one-side power spectral density. $\mathbf{I_{MP}}$ is the identity matrix of order MP. The multipath channel response is a matrix of dimension MP by P+L-1:

$$H_k = \begin{vmatrix} \mathbf{H}_k & \mathbf{0} & \cdots & \mathbf{0} \\ \mathbf{0} & \mathbf{H}_k & \cdots & \vdots \\ \vdots & \vdots & \ddots & \mathbf{0} \\ \mathbf{0} & \cdots & \mathbf{0} & \mathbf{H}_k \end{vmatrix}, \qquad (8)$$

where $\mathbf{0}$ is a M×1 all-zero vector [3, pp. 87].

The cross-correlation between the *k-th* user's symbol sequence and the whole received signal is given by:

$$\mathbf{p}_k = H_k \mathbf{e}_P = H_k^{(P)}\,, \qquad (9)$$

where $\mathbf{e_P}$ is a column vector of dimension (P+L-1) with ones at the *P-th* position and zeros elsewhere, and $H_k^{(P)}$ indicates the *P-th* column of H_k.

The signal covariance matrix for the *k-th* target user, with dimension MP by MP, is given by:

$$\mathbf{R}_{\mathbf{s},k} = \mathbf{p}_k \mathbf{p}_k^H\,. \qquad (10a)$$

Therefore, the MAI plus noise covariance matrix observed by the k-th user is given by: $\mathbf{R}_{u,k} = \mathbf{R} - \mathbf{R}_{s,k}$. (10b)

Using the Wiener-Kolmogorov theory, the $\mathbf{W}_k$ that minimizes the MSE at 2D Rake receiver output is given by:

$$\mathbf{W}_{ot,k} = \mathbf{R}^{-1}\mathbf{p}_k\,. \qquad (11)$$

Using the Woodbury's identity (or matrix inversion lemma) to $\mathbf{R}^{-1}$ ($\mathbf{R}$ is given by Eq. 7), then the maximum SINR solution for the *k-th* user can be stated as:

$$\mathbf{W}_k = \beta \mathbf{R}_{\mathbf{U}_k}^{-1}\mathbf{p}_k\,, \qquad (12)$$

where β is a scale constant which does not affect the SINR, as it equally applies to all signals.

Using (12) in (1), the SINR can be rewritten as:

$$SINR = G_p\, \mathbf{p}_k^H \mathbf{R}_{\mathbf{U}_k}^{-1}\mathbf{p}_k\,. \qquad (13)$$

Finally, we have observed that the Liu's definition for the SINR (where MMSE is the minimum MSE at the 2D Rake receiver output [2, pp. 89-93]), i.e.

$$SINR = \frac{1}{MMSE} = 1 + G_p\, \mathbf{p}_k^H \mathbf{R}_{\mathbf{U}_k}^{-1}\mathbf{p}_k\,, \qquad (14)$$

is only valid if $G_p \mathbf{p}_k^H \mathbf{R}_{\mathbf{U}_k}^{-1}\mathbf{p}_k >> 1$.

III – Maximum Ratio Combining Receiver

In this section, we have assumed the following: *(i)* a receiver with M antennas and P taps per antenna which response is obtained by the MRC or coherent solution; *(ii)* the MAI is modelled as a flat power spectrum density and all received signals have the same average power; *(iii)* the fading is independent in all antennas (i.e. M_D=M). As trace of a scalar is a scalar itself, then the SINR (Eq. 1) can be rewritten as:

$$SINR_k = \frac{G_p\, tr(\mathbf{p}_k^H \mathbf{R}_{s,k} \mathbf{p}_k)}{E\left[tr(\mathbf{p}_k^H \mathbf{R}_{u,k} \mathbf{p}_k)\right]}\,, \qquad (15)$$

where tr(**A**) denotes the trace of matrix **A**, and $\mathbf{W}_k = \mathbf{p}_k^*$ due to MRC assumption (* denotes the complex conjugate). Assuming that the received signals at the antenna array are spatially and temporally white and that the receiver diversity is matched with the channel inbound diversity (i.e. P=L), we have the following:

$$\mathbf{R}_{\mathbf{s},k} = \mathbf{I}_{MP}\,, \qquad (16a)$$

$$\mathbf{R}_{u,k} \cong KL(1+f)\,\mathbf{I}_{MP} + \sigma_n^2 \mathbf{I}_{MP}, \qquad (16b)$$

where f is the relative other-cell interference factor [6, pp. 189]. Finally,

$$SINR_k = \frac{G_p\, tr(\mathbf{p}_k \mathbf{p}_k^H \mathbf{R}_{s,k})}{E\left[tr(\mathbf{p}_k \mathbf{p}_k^H \mathbf{R}_{u,k})\right]} \approx \frac{G_p \sum_{m=1}^{MP} |\alpha_{k,m}|^2}{(1/P)KL(1+f)}\,, \qquad (17)$$

where the AWGN was neglected due to interference limited assumption. Notice that the factor 1/P=1/L in the denominator comes from (5). It was also used that the trace of matrix product **AB** equals the trace of matrix product **BA**.

If the magnitude of multipath fading is supposed to be a Nakagami-m RV, we can verify the SNIR probability density function (PDF) at the output of the MRC 2D Rake receiver is of Gamma kind with shape parameter β equals to MPm [7] :

$$p(x) = \begin{cases} \dfrac{1}{\Gamma(\beta)} \left(\dfrac{m}{\overline{SINR}}\right)^{\beta} (x)^{\beta-1} \exp\left(-\dfrac{mx}{\overline{SINR}}\right) & \text{if } x>0,\ m \geq 0.5, \\ 0 & \text{elsewhere} \end{cases} \qquad (18)$$

where Γ(z) is the gamma function and

$$\overline{SINR} \cong \frac{(1/P)G_p MP}{(1/P)KL(1+f)} = \frac{G_p MP}{KL(1+f)}\,, \qquad (19)$$

Notice that the PDF of SINR at the output of a receiver with just one antenna and one finger is also Gamma, but with β equals to m (the Nakagami-m fading figure). Finally, we have noticed that the Gamma RV degenerates in a impulse function when $\beta \to \infty$.

Evidently, the 2D RAKE receiver reduces to an antenna array (AA) receiver if the number of filter taps per antenna, P, is set to one. Considering an LES AA receiver on a flat fading channel correlated in all antenna elements, then the spatial signature is given by:

$$\mathbf{h}_k = \sqrt{P_k}\,\alpha_k \left[1 \; e^{j\pi\sin\theta_k} \cdots e^{j(M-1)\pi\sin\theta_k}\right]^T. \qquad (20)$$

Therefore, a coherent combining receiver has a normalized response given by:

$$\mathbf{W}_k^H = \sqrt{P_k}\,\alpha_k^* \left[1 \; e^{-j\pi\sin\theta_k} \cdots e^{-j(M-1)\pi\sin\theta_k}\right] / \left(\|\mathbf{h}(\theta_k)\|\right), \quad (21)$$

where $\|\mathbf{h}_k\|$ is the Euclidian norm of the steering vector $\mathbf{h}_k$.

Modeling the MAI as a flat power spectrum, then the normalized MAI interference at AA output can be stated as [8, pp. 151]:

$$\frac{I}{K(1+f)} = \frac{E[P|\alpha|^2]}{M} \sum_{m=0}^{M-1}\sum_{n=0}^{M-1} E[e^{-j\pi(n-m)\sin\theta}]\, E[e^{j\pi(n-m)\sin\phi}], \quad (22)$$

where θ and ϕ are RVs that model the DOA at the azimuth direction. Correspondingly, assuming perfect power control, the average SINR is given by:

$$\overline{SINR} \approx G_p \frac{M}{\frac{K(1+f)}{M}\sum_{m=0}^{M-1}\sum_{n=0}^{M-1} E[e^{-j\pi(n-m)\sin\theta}]\, E[e^{j\pi(n-m)\sin\phi}]}, \qquad (23)$$

where the AWGN was neglected. We have noticed that the jargon *pole point* or *pole capacity* is used to designate the capacity that cannot be reached (due to perfect PCL and negligible AWGN assumptions), but which serves as a useful reference point for network planners.

IV - Network Simulator

The main characteristics of the system level simulator with full interactivity between all cells are [5]:

- The network consists of a homogenous hexagonal macrocellular network with N_{BS} ideal three-sectored cells.
- The MSs are uniformly distributed over the cells.
- The long-term paths loss is log-linear with the propagation exponent Γ set to 4. The shadowing is modelled by a Gaussian RV in dB (or log-linear RV in linear scale) with zero mean and standard deviation σ_{dB} set to 8 dB.
- The DOA of each discrete multipath are uniformly $[\overline{\theta}_k - 5^\circ, \overline{\theta}_k + 5^\circ]$ distributed, where the mean DOA $\overline{\theta}_k$ is uniformly distributed in each sector (i.e. between -60^0 and $+60^0$ in sector 0 and so forth).

V - Simulation Versus Analytical Results

In figures 1 to 3, it is assumed an equal strength (ES) Rayleigh frequency selective fading channel with 3 taps, i.e. L=3. In this section, the Signal-to-Noise Ratio (SNR) has been set to 100 dB, i.e. an interference limited system has been considered.

As a direct consequence of the law of large numbers, Fig. 1 shows that the similitude between analytical and simulation results increases with the channel load.

Besides evidencing the larger effects of spatial diversity on the system performance, Fig. 2 also ratifies the excellent agreement between simulation and analytical results.

Theoretically it is expected that the intercell MAI reduces the capability of the optimum 2D RAKE receiver in canceling the interference. Consistently, Fig. 3 shows that the performance gain of the optimum 2D Rake receiver in relation to the MRC 2D Rake receiver diminishes considerably when the intercell MAI is taken into account. The other cell interference factor f was set to 0.6 to estimate the analytical response when it is assumed a cellular system 19 BSs.

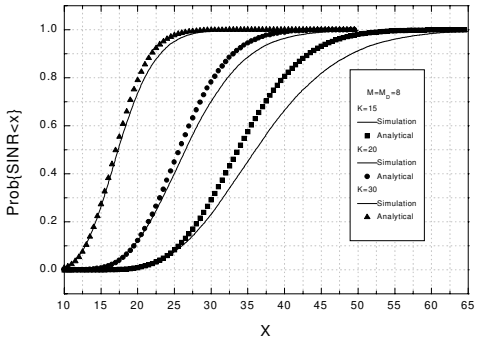

Fig.1. Comparison, parameterized by the channel load K, between analytical and simulation results for the MRC 2D Rake receiver. N_{BS}=1; G_p=64; L=P=3.

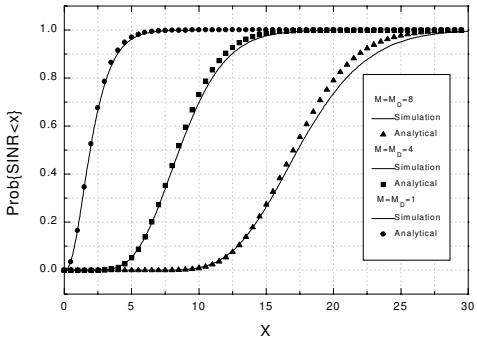

Fig. 2. Comparison, parameterized by the number of antennas M, between analytical and simulation results for the MRC 2D Rake receiver. N_{BS}=1; K=30; G_p=64; L=P=3.

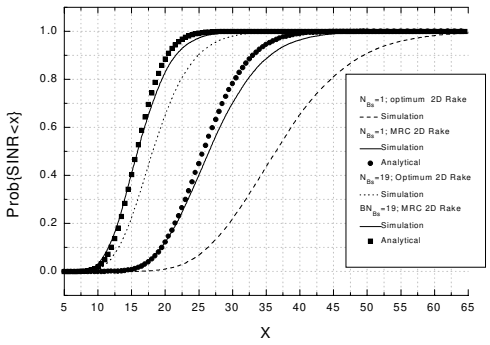

Fig. 3. Effects of intercell MAI on the performance of the optimum 2D Rake receiver and MRC 2D Rake receiver. M=M_D=8; L=P=3. K=20; G_p=64; Γ=4, σ_{dB}=8 dB.

It is well-known that the Nakagami-m RV reduces to a Rayleigh and exponential negative distribution when the fading figure m is set to 1 and 0.5, respectively. The Nakagami-m RV can also model a Ricean fading with factor K_{rice} if m is set to $(1+K_{rice})^2/(1+2K_{rice})$ [9, pp.43]. Fig.

4 shows that spatial and temporal processing of 2D Rake receiver reduces the effects of fading figure m on the system performance. This figure also shows that the performance of the MRC 2D Rake receiver approximates the performance obtained with the optimum 2D Rake receiver when the channel load increases.

For uniformly distributed DOA, Tab. 1a shows: *(i)* a good agreement between numerical (equations 22 and 23) and simulation results; *(ii)* a sensible reduction of system performance in hot spot scenarios. Analysing Tab. 1b we can infer the following: *(i)* the performance gain due to optimum SINR solution (Eq. 12) reduces considerably when the AA becomes severely overloaded; *(ii)* both receivers lead to a gain of 3 dB in the average SINR when the processing gain is doubled.

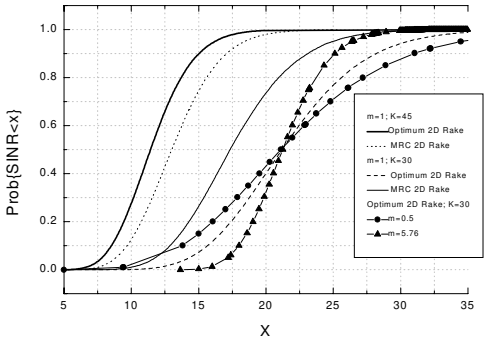

Fig. 4. Effects of channel load and Nakagami´s fading figure on the system performance.
N_{BS}=1; G_p=64 ; M=M_D=8; L=P=3.

Tab. 1. AWGN channel with perfect power control loop. M=8, M_D=1; E[$|\alpha|^2$]=1; SNR=100 dB. N_{BS}=19; f=0.6

Tab 1a. Effects of DOA on the system performance. G_p=64; K=40

	Numerical		Simulation		
DOA	Norm MAI	Mean SINR	Norm. MAI	Mean SINR	Median SINR
U[-10^0,10^0]	4.2	2.9 dB	3.8	3.6 dB	3.2 dB
U[-20^0,20^0]	2.4	5.2 dB	2.5	5.3 dB	5.0 dB
U[-30^0,30^0]	1.8	6.6 dB	1.8	6.8 dB	6.5 dB
U[-60^0,60^0]	1.1	8.7 dB	1.1	9.0 dB	8.8 dB

Tab 1b. Effects of channel load on the mean SINR in dB. DOA is uniformly distributed between U[-60^0,60^0]

	Numerical		Simulation			
	G_p=32	G_p=64	G_p=32		G_p=64	
K	MRC	MRC	MRC	2D Rake	MRC	2D Rake
10	12.0	15.0	13.1	15.8	16.1	18.8
20	8.8	11.8	9.3	10.9	12.3	13.9
40	5.7	8.7	6.0	6.9	9.0	10.0

The results shown in this section are minor samples of the extensive efforts carry out in order to validate [10] a packet network simulator that has been developed in C^{++} using object oriented paradigm approach. From this point on, since the analytical results presented are based upon some specific postulates (e.g. MRC receiver), we will use simulation to assess the optimum 2D Rake receiver performance.

VI - Soft Handoff

The external interference in the target cell can be modelled as a sum of two components [6, pp. 189]:

$$I_{ext} = I_{S_0} + I_{\bar{S}_0}, \quad (24)$$

where I_{S_0} denotes the component of external interference originated in the region where the MS can be controlled by the target cell. Correspondingly, $I_{\bar{S}_0}$ is the complementary region of I_{S0}. Assuming an MS located at the central cell, Fig. 5 exemplifies these two regions for N_c=1, 2, 3, 4 and 9. Notice that N_c, determined by the criterion of minimum distance, is the number of BSs qualified to assume the control of MSs located at the central cell.

In the previous results, it was used a perfect instantaneous handoff, i.e. the MSs were always logically connected with the BS for which the average path loss in the downlink is minimum. Notice that in this case $I_{\bar{S}_0} = 0$.

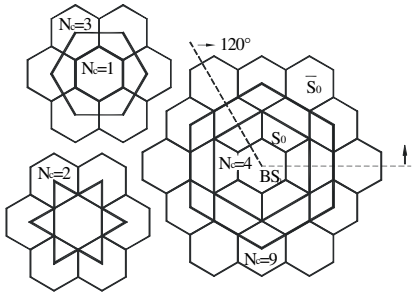

Fig. 5.Illustration of regions S_0 and $\bar{S}_0$ for N_c=1, 2, 3, 4 e 9.

In this section it has been considered an ES Rayleigh frequency selective fading channel with 3 taps.

Fig. 6 shows the effects of number of preferential cells, N_c, on the throughput. The throughput is calculated as

$$\eta = \sum_{k=0}^{K-1} k p_K(k), \quad (25)$$

where $p_K(k)$ is the probability of k packets being acknowledged (ACK) at the BS when the channel is loaded with K packets. The packet is ACK if the SINR at the receiver output is greater than a threshold $SINR_0$. Observe in Fig. 6 that if the path loss exponent and the standard deviation are set to 3 and 12 dB, respectively, it is expected a considerable performance degradation when N_c is not set to 19. The above characteristics occur due to the excess of the intercell interference generated in the region $\bar{S}_0$. However, if the path loss exponent and the standard deviation are set to 4 and 8 dB, respectively, then the path loss attenuates the intercell interference generates in the region $\bar{S}_0$ and thus the performance loss is not so relevant. Therefore, we have concluded that in order to avoid a strong dependence of system performance with the radio propagation environment, it is necessary, even with the advanced 2D Rake receivers, an well-optimized pilot search mechanism in such way that the MSs transmit the minimum possible average power.

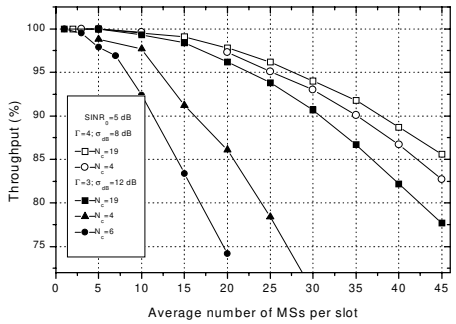

Fig 6. Effects of N_c on the throughput of a cellular system with 19 BSs. G_p=64; M=8, M_D=1; L=P=3; SNR=10 dB.

When in soft handoff, the MS is connected to N_{soft} BSs, and the selection diversity is implemented on a frame basis, that is, the better frame received by either BSs is accepted by the network. To investigate the effects of soft handoff, it is assumed that: *(i)* all MSs are in soft handoff state; *(ii)* the MSs are power controlled by the BS in which there is a lesser attenuation in the downlink.

Figures 7a, for Γ=4 and σ_{dB}=8 dB, and 7b, for Γ=3 and σ_{dB}=12 dB, show that when the channel is lightly loaded the soft handoff allows improvement between 1.0 and 1.5 dB in the SINR statistics observed at the 2D Rake receiver output. We also noticed a negligible additional gain when more of two BSs are involved in the soft handoff.

Supposing it is feasible to implement soft handoff with MRC tenchique, Fig. 8 shows that the soft handoff allows gains around of 2 dB in SINR observed at the 2D Rake receiver output.

In *cdmaOne* systems, for instance, the power control of MSs in soft handoff is distributed, i.e. the MS only increases its transmitted power if all BSs involved in soft handoff order to. Otherwise, the transmitted power is decreased. Notice that the distributed power control reduces the intercell MAI. In this paper it has been assumed that the MSs are power controlled by the BS with lesser attenuation in the downlink, so we can expect that the soft handoff with distributed power control allows gains still more significant in relation to those ones showed in this section (e.g. in the link budget of WCDMA systems it has been assumed a soft handoff gain of 3 dB).

VII - MaxMin SINR Scheduling Scheme

The dynamic allocation scheme aims loading each time slot with MSs that have their spatial signatures with low cross-correlation and, as a consequence, it increases the SINR at the input of the detection circuit. In order to accomplish an investigation on the scheduling effects on the system performance, it is assumed that: *(i) S* MSs are physically located at each BS of a TDD DS-CDMA system with N_{slots} time slots per uplink frame; *(ii)* each BS acquires and broadcasts information to the MSs using a MAC pooling protocol [11]; *(iii)* the channel transfer function for all MSs is known at each BS; *(iv)* the channel transfer function remains constant between

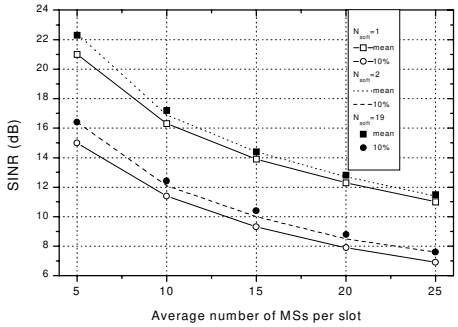

Fig. 7a. System with 19 Bs with Γ=4 and σ_{dB}=8 dB.

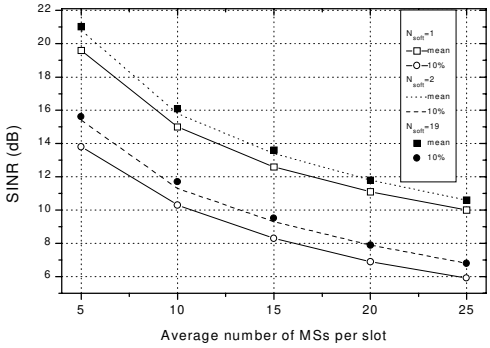

Fig. 7b. System with 19 BSs with Γ=3 and σ_{dB}=12 dB.

Fig 7. Effects of *soft handoff with selection diversity* on the SINR statistics.
N_c=19; G_p=64; M=8, M_D=1; L=P=3; SNR=10 dB.

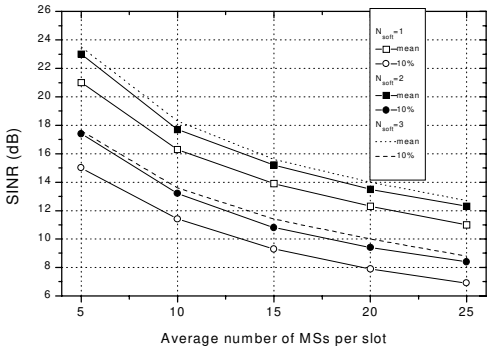

Fig 8. Effects of *soft handoff with MRC* on the SINR statistics of a cellular system with 19 BSs. N_c=19; Γ=4; σ_{dB}=8 dB. G_p=64; M=8, M_D=1; L=P=3; SNR=10 dB.

the beginning of the polling period and the end of the last data uplink time slot.

The MSs scheduling on the time slots is accomplished as follows: (1) the first N_{slots} MSs are allocated to each slot; (2) each additional MS is assigned to the slot *n* if the MaxMin SINR metric is satisfied; (3) steps 2 and 3 are repeated until all MSs are assigned. In the *MaxMin* $SINR_{thr}$ metric, the step two of the previous section is accomplished as follows: the proving MS is hypothetically allocated in all time slots and the SINR is estimated for the proving MS and all MSs already allocated in each time slot. The MS is definitely scheduled to the slot if the largest minimum SINR among

all slots is greater than the $SINR_0$. The following results refer a Rayleigh frequency channel with L=3.

Figures 9a and 9b show the effects of number of spatial diversity branches on the throughput when the $SINR_0$ is set to 5 dB and 8 dB, respectively. These figures show that the *MaxMin SINR* scheduling scheme allows an expressive improvement on the throughput in single-cell systems. It has also been noticed that the spatial diversity increases substantially the throughput, mainly in systems without scheduling. Finally, notice that the spatial diversity has a greater effect on the throughput when the $SINR_0$ is reduced from 8 dB to 5 dB, i.e. when the users demand a less quality-of-service (QoS).

Figures 10a and 10b show the effects of scheduling and soft handoff (with selection diversity) on the SINR statistics and throughput, respectively, of a cellular system with seven BSs. These figures show that when the scheduling is implemented, the improvement of soft handoff on the performance is not so relevant.

Comparing Fig. 10b with Fig. 9, we have verified that, albeit still substantial, the intercell interference reduces the scheduling effects on the system performance. This characteristic occurs due to the other-cell interference observed in the scheduling period is uncorrelated with the external MAI noticed in the traffic time slots.

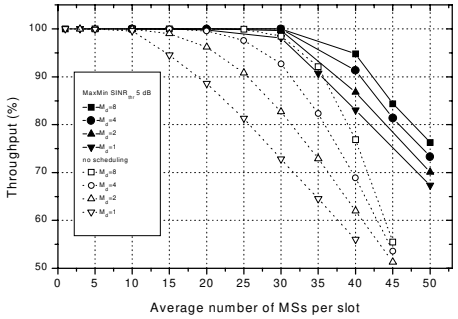

Fig 9a. $SINR_0$= 5 dB.

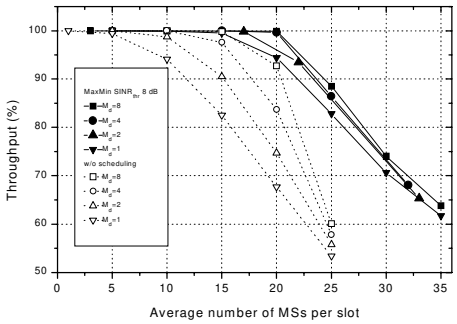

Fig 9b. $SINR_0$= 8 dB.

Fig 9: Effects of number of spatial diversity branches on the throughput in a single cell system. G_p=16, M=8, L=P=3.

VIII – Conclusions

Among of analytical results derived, remarks and conclusions that were done in the earlier sections, we emphasize that the dynamic time slot scheduling schemes can provide substantial improvements on the performance of TDD DS-CDMA systems with 2D Rake receivers. We also have shown that it is necessary to implement distributed power control in order to maximize the gains due to soft handoff.

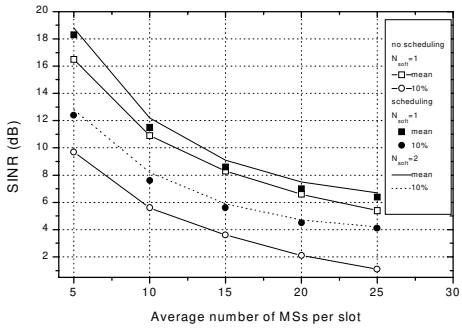

Fig 10a. SINR statistics

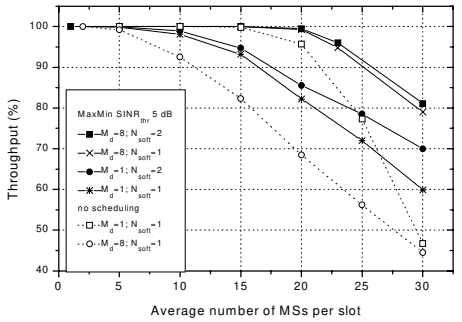

Fig 10b. Throughput. $SINR_0$= 5 dB.

Fig 10. Effects of scheduling and soft handoff on the performance of a cellular system with 7 BSs
$SINR_0$= 5 dB; G_p=16; M=8, M_D=1; L=P=3, SNR=10 dB.

References

[1] R. P. F. Hoefel, and C. de Almeida, "Single packet transmission and multislot scheduling for WWW packet transmission in a TDD DS-CDMA multicellular network with a broadband adaptive receiver," in *Proc. of 11th Virginia Tech/MPRG Symposium on Wireless Personal Communications,* pp. 205-216, 2001.

[2] R. P. F. Hoefel. "On the Performance of a Joint TDD CDMA/PRMA and CDMA/ALOHA Protocols with 2D RAKE receivers in Single-Cell and Multi-Cell Networks", *IEEE VTC Fall 2001, Atlantic City, USA, 2001.*

[3] H. Liu. *Signal Processing Applications in CDMA Communications*, Artech-House, 2000.

[4] J. Litva and T. K-Y. Lo. *"Digital beamforming in wireless communication*". Artech-House, 1996.

[5] R. P. F. Hoefel, and F. R. P. Cavalcanti. "Performance evaluation of a SDMA MAC protocol using broadband adaptive antennas over a multicellular environment," *Proc.of IEEE Conference on Third Generation Mobile Communications*, San Francisco, USA, June 2001.

[6] A. J. Viterbi. *"CDMA: principles of spread spectrum communication",* Addison-Wesley, 1995.

[7] R. P. F. Hoefel, C. de Almeida. "The Performance of CDMA/PRMA for Nakagami-m Frequency Selective Fading Channel". *Electronics Letters*, 35 (1): 28-29, Jan. 1999.

[8] J. C. Liberti, T. S. Rappaport. *Smart Antennas for Wireless Communication.* Prentice Hall, 1999.

[9] R. Prasad. *Universal wireless personal communications,* Boston: Artech House, 1998.

[10] K. Pawlikowski, H-D J. Jeong and J-S R. Lee, "On credibility of simulation results of telecommunications networks, " *IEEE Communications Magazine*, vol. 40, no. 1, pp. 132-139, Jan. 2002.

[11] M. Zorzi. "Performance of a MAC protocol with smart antennas in a multicellular environment", *Proc. IEEE Int. Conf. Communications (ICC'2000),* , USA, 2000, pp. 402-407.